Journal of Alloys and Compounds 509 (2011) 1722–1728

Contents lists available at ScienceDirect

Journal of Alloys and Compounds

journal homepage: www.elsevier.com/locate/jallcom

Microstructural behavior of the heat treated n-type 95% Bi_2Te_3–5% Bi_2Se_3 gas atomized thermoelectric powders

Mahedi Hasan Bhuiyan [a], Taek-Soo Kim [b], Jar Myung Koo [a], Soon-Jik Hong [a,*]

[a] Division of Advanced Materials Engineering, Kongju National University, 275, Budae-dong, Cheonan City, Chungcheongnam-do, 330-717, Republic of Korea
[b] Korea Institute of Industrial Technology (KITECH), 7-47, Songdo-dong, Yeonsu-Gu, Incheon 406-840, Republic of Korea

ARTICLE INFO

Article history:
Received 11 June 2010
Received in revised form 2 October 2010
Accepted 6 October 2010
Available online 16 October 2010

Keywords:
Thermoelectric material
Powder metallurgy
Gas atomization
Heat treatment
Microstructure

ABSTRACT

In this research, n-type 95% Bi_2Te_3–5% Bi_2Se_3 doped with 0.04% SbI_3 thermoelectric powders were manufactured by gas atomization process and subsequently, the effects of rapid solidification and heat treatment on the microstructure of the powder particles were investigated. The crystal structures were analyzed by X-ray diffraction (XRD) and cross-sectional microstructures were observed by the scanning electron microscopy (SEM). The rapidly solidified powders consist of homogeneously distributed needle shape intermetallic compounds. However, the size of the intermetallic compounds increased with the increasing powder size, whereas the oxygen content in the produced powder decreased. Heat treatment of the powders for various temperatures and periods showed a significant increase in the grain size resulting in a reduction in hardness. In addition, with the increasing heat treatment temperatures and periods, the orientation factor of the powder particles decreased, which is also evident in case of the reduction treated powders.

1. Introduction

The exclusive advantages of thermoelectric cooling module such as small size and weight, spot cooling system, no moving parts and noise, precise temperature control and environment friendly etc. compared with the mechanically operated refrigeration systems [1] have recently drawn a considerable attention in this research field among the scientists and researchers all over the world. Due to good figure-of-merit operating at the region of room temperature, Bi_2Te_3 and its related ternary alloys [2], such as consisting of Bi_2Te_3 with either Bi_2Se_3 or Sb_2Te_3, are the leading thermoelectric materials have long been used for thermoelectric cooling. The crystal structure of Bi_2Te_3 is rhombohedral [3] and shows anisotropic properties [4]. These materials can be prepared by a number of ways, like directionally grown single crystals [5], powder metallurgy techniques [6] and thin films technology [7]. Although directionally grown single crystals are more favorable to use commercially as they exhibit the highest figure of merit [5], the poor mechanical properties due to coarse grain size and easily occurring fractures along the Te(1)–Te(1) cleavage planes, account for material wastage to some extent during the fabrication process of the modules, accompanied by a decrease in the reliability level of the modules during practical applications. On the other hand, fabrication of materials through powder metallurgy technique provides higher compressive strength as well as simultaneous increase in the figure of merit [6] as a result of grain refinements and reduction in lattice thermal conductivity. The required powder can be produced by gas atomization [6], mechanical alloying [8], chemical reactions [9] as well as some other special methods depending on the material, economy and their applications. Among all of these, the gas atomization became attractive due to its efficient and high performance application, easy process control, mass production rate and homogeneous productivity without segregation relative to other manufacturing processes. In powder metallurgy system, materials in the form of powders are usually compacted through extrusion [6], hot pressing [8], spark plasma sintering (SPS) [10] and plasma activated sintering (PAS) [11] to acquire fine microstructures with unique properties. These consolidation processes involve high temperature applications affecting the microstructure of the bulks, and thus altering mechanical and thermoelectric properties. As the mechanical and thermoelectric properties are largely dependent on the microstructures, and the microstructure formation is influenced by the hot consolidation processes, therefore it is an urgent need to analyze and establish the relationships between the material processing parameters, microstructures and their properties, facilitating a full control over the processes in terms of properties. Accordingly, investigation of the heat treated powders can be considered as a pre-requisite and inevitable step that should be accomplished prior to the processing's, in order to understand microstructural behavior of the powders subjected to high temperatures during consolidation processes. Despite a lot of researches were conducted previously on Bi_2Te_3 powders produced by gas

* Corresponding author. Tel.: +82 41 521 9387; fax: +82 41 568 5776.
E-mail address: hongsj@kongju.ac.kr (S.-J. Hong).

0925-8388/$ – see front matter © 2010 Elsevier B.V. All rights reserved.
doi:10.1016/j.jallcom.2010.10.021

atomization and/or milling processes, however, none of those elaborately reported powder characterization and its property variation depending on the heat treatment temperatures as well as the holding time. Hence, the essence of this research represents microstructural investigation of 95% Bi_2Te_3–5% Bi_2Se_3 doped with 0.04% SbI_3 gas atomized powders as a function of various heat treatment conditions.

2. Experimental procedure

High purity (>99.999%) elementary Bi, Te and Se granules were weighed for the required stoichiometric composition of 95% Bi_2Te_3–5% Bi_2Se_3 doped with 0.04% SbI_3 alloy, and placed at a high density graphite crucible in an induction furnace evacuating at 4.4 mTorr. The alloy was melted and superheated 200 °C above the liquidus temperature under Ar atmosphere to make the master alloy, and then bottom pouring the melt through a boron nitride melt delivery nozzle of 8 mm diameter to a N_2 gas operated atomizer working at a pressure of 1.2 MPa, the rapidly solidified powders were produced. The size distribution of the as-atomized powders was carried out by laser diffraction technique using Mastersizer 2000 particle size analyzer. To examine the effect of rapid solidification on the microstructure of the powders, the conventional mechanical sieving method was employed to classify the as atomized powders into small (~45 μm), medium (75–106 μm) and large (180–250 μm) size range. The oxygen content of the powders was determined by the equipment of Eltra ONH-2000 Oxygen/Nitrogen/Hydrogen determinator. In order to understand the effect of high temperature on the microstructures, powders of 65–80 μm size range were heat treated at 300, 350, 400 and 500 °C temperatures for 1, 3 and 5 h. The as atomized powders were also reduced at 360 °C for 4 h under 10% H_2 atmosphere. Crystal structures of the as-atomized, reduction treated and heat treated powders were characterized by X-ray diffractometer (XRD) using high energy monochromatic CuKα radiation (15.418 nm) in the 2θ range from 10 to 70° at a scan rate of 0.05°/s. The morphology and cross-sectional microstructure of the powders were observed by the scanning electron microscopy (SEM) after polishing and etching by a solution of HNO_3 and H_2O in the ratio of 1:1 for 5 s. Vickers hardness of the powder was measured by the Vickers hardness tester applying the load of 98.07×10^{-3} N for 15 s, and the values were averaged.

3. Results and discussion

Fig. 1 represents SEM micrograph showing typical morphology of 95% Bi_2Te_3–5% Bi_2Se_3 doped with 0.04% SbI_3 gas atomized powders in different size range. All the small (~45 μm), medium (75–106 μm) and large (180–250 μm) size powder particles were spherical in shape. It is much desirable to obtain such kind of particles as shown in Fig. 1, since spherical powders with smooth surfaces and fewer satellites contribute to higher packing density and free flowing characteristics. The log normal and cumulative size distribution of the gas atomized powders are illustrated in Fig. 2(a) and (b). A broad and bimodal size distribution of the powders could be observed in Fig. 2(a). The surface weighted mean and volume weighted mean of the particles were 14.13 μm and 68.431 μm, respectively. Generally, gas atomization process results in a wide range of particle size due to variation in the cooling rate, which is inversely proportional to the size of the liquid droplets. Furthermore, bimodal size range of the powders improves the packing density comparing to the monosized powders [12] during the compaction processes, as the smaller particles can easily place themselves at the interstitial positions of the gaps between the larger particles, and thus reducing the voids within the powder particles provides a significant increase in the final density. The cumulative size distribution in Fig. 2(b) indicates D_{10} = 7.291 μm, D_{50} = 22.252 μm and D_{90} = 220.03 μm corresponding to the particle sizes at 10%, 50% and 90%, respectively. The standard deviation was calculated using the equation, $\sigma = \ln(D_{84}/D_{50})$ and found to be 1.91 μm. That means 68% powders fall between 20.34 μm and 24.16 μm, whereas 95% powders have a size range between 18.43 μm and 26.07 μm on volume basis. Since, the thermoelectric and mechanical properties of the bulk depend on the microstructure, and the microstructure is affected by the initial powder size, therefore, the demand of narrow size distribution of powders is gradually increasing. It is expected that an improvement in the design parameters and process parameters of gas atomization would deliver high quality powders, significantly reducing the volume median diameter D_{50} to the finer particle sizes.

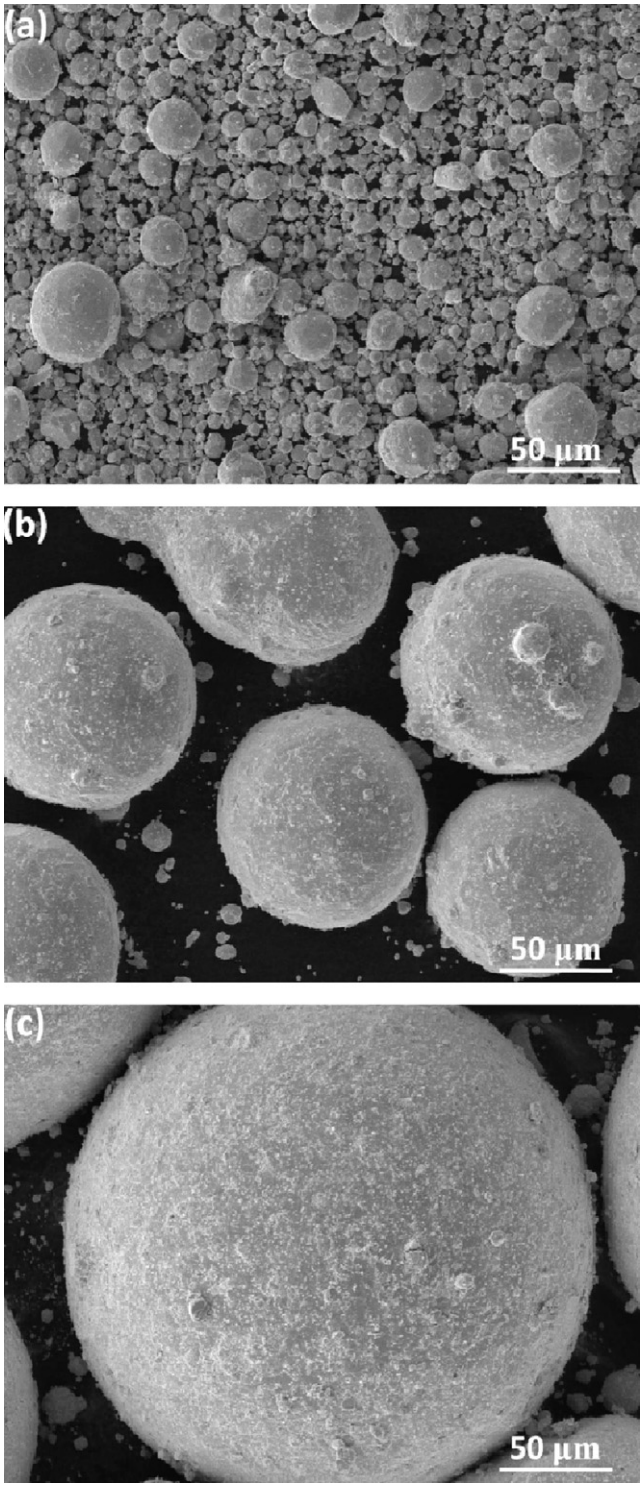

Fig. 1. Morphology of the gas atomized 95% Bi_2Te_3–5% Bi_2Se_3 powders (a) ~45 μm (b) 75–106 μm and (c) 180–250 μm.

The powder fabrication procedure often contaminates the powder by adsorbing oxygen as a film on its surface. Fig. 3 demonstrates the oxygen content of 95% Bi_2Te_3–5% Bi_2Se_3 gas atomized powders according to different size range. It appears that the maximum oxygen content of 240.60 ppm was obtained in the small size (~45 μm) powders due to its high specific surface area. However, with the increasing powder size to medium (75–106 μm)

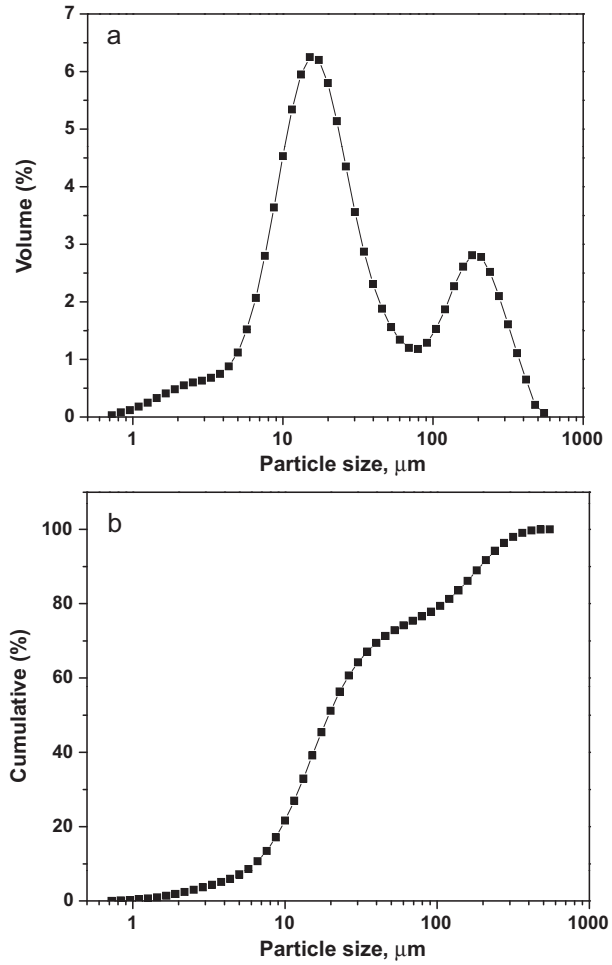

Fig. 2. Log normal size distribution (a) and cumulative size distribution (b) of gas atomized 95% Bi_2Te_3–5% Bi_2Se_3 powders.

and large (180–250 μm) particles, the oxygen content decreased to 137.47 ppm and 78.97 ppm, respectively. Although oxidation of the powders may reduce the interparticle friction, the thermoelectric performance is substantially degraded by its presence. The formation of oxide layer passivates the powder surfaces interrupting the electrical transportation systems, and results in a reduction in the electrical conductivity of the material. Moreover, investigating the effect of oxygen content on the microstructure [13] reveals that alloys containing higher oxygen, exhibit low carrier mobility and comprise second phase inclusions in the grain boundaries, inhibiting grain growth during high temperature consolidation processes. Therefore, in order to attain a high figure-of-merit, controlling the ambient condition to minimize the oxygen content is a great concern during powder synthesis process. The figure-of-merit (Z) of a thermoelectric material can be defined as:

$$Z = \frac{\alpha^2 \sigma}{\kappa} \quad (1)$$

where, α is the seebeck coefficient, σ is the electrical conductivity and κ is the thermal conductivity of the material. Manufacturing of Bi_2Te_3–Bi_2Se_3 thermoelectric materials through various techniques generally yields stoichiometric compounds like Bi_2Te_3, Bi_2Se_3 and $Bi_2(TeSe)_3$ phases regarded as congruent for thermoelectric operations [14] accompanied by a number of incongruent BiTe, BiSe, Bi_2Te and Bi_2Se phases caused by peritectic reactions during their solidification processes, and the formation of such undesirable incongruent compounds could be avoided by rapid solidification of the powders [15]. Consequently, the crystal structures of 95% Bi_2Te_3–5% Bi_2Se_3 gas atomized powders were observed from the XRD traces as shown in Fig. 4. XRD pattern of the as atomized powders confirmed the presence of Bi_2Te_3 phase with rhombohedral crystal structure (space group $R3m$) having lattice parameters of a = 4.395 A and c = 30.44 A. In addition, the intensity and width of the main peak both increased with the decreasing powder size, indicating rapid solidification of the powders along with microstrucutural refinement. Alloying of various elements is effective in reducing lattice thermal conductivity through alloy scattering mechanism resulting in high figure-of-merit.

To study the influence of rapid solidification on the microstructure, the cross-sectional microstructure of 95% Bi_2Te_3–5% Bi_2Se_3 powders was observed by SEM as represented in Fig. 5. As can be seen from the micrographs, a homogeneous and uniformly distributed needle shape intermetallic compounds were present in the powders, and with the increasing powder size, the width of the needle shape increased, especially it is noticeable in case of the large particles (Fig. 5(c)). For small size (~45 μm) powders, the average width of the grain was around 1.5 μm, and the grain size increased to about 2–4 μm and 6–8 μm for the medium (75–106 μm) and

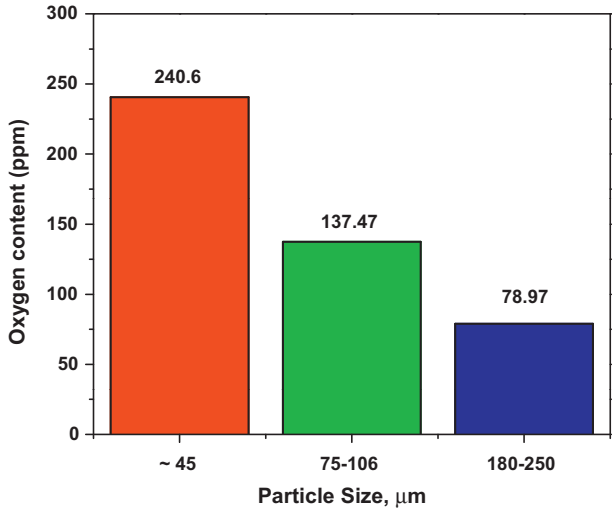

Fig. 3. Oxygen content of 95% Bi_2Te_3–5% Bi_2Se_3 gas atomized powders according to the powder size.

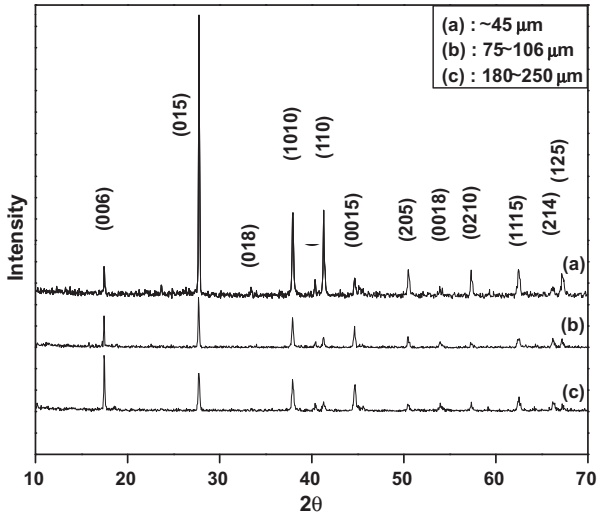

Fig. 4. XRD patterns of the 95% Bi_2Te_3–5% Bi_2Se_3 gas atomized powders according to the powder size.

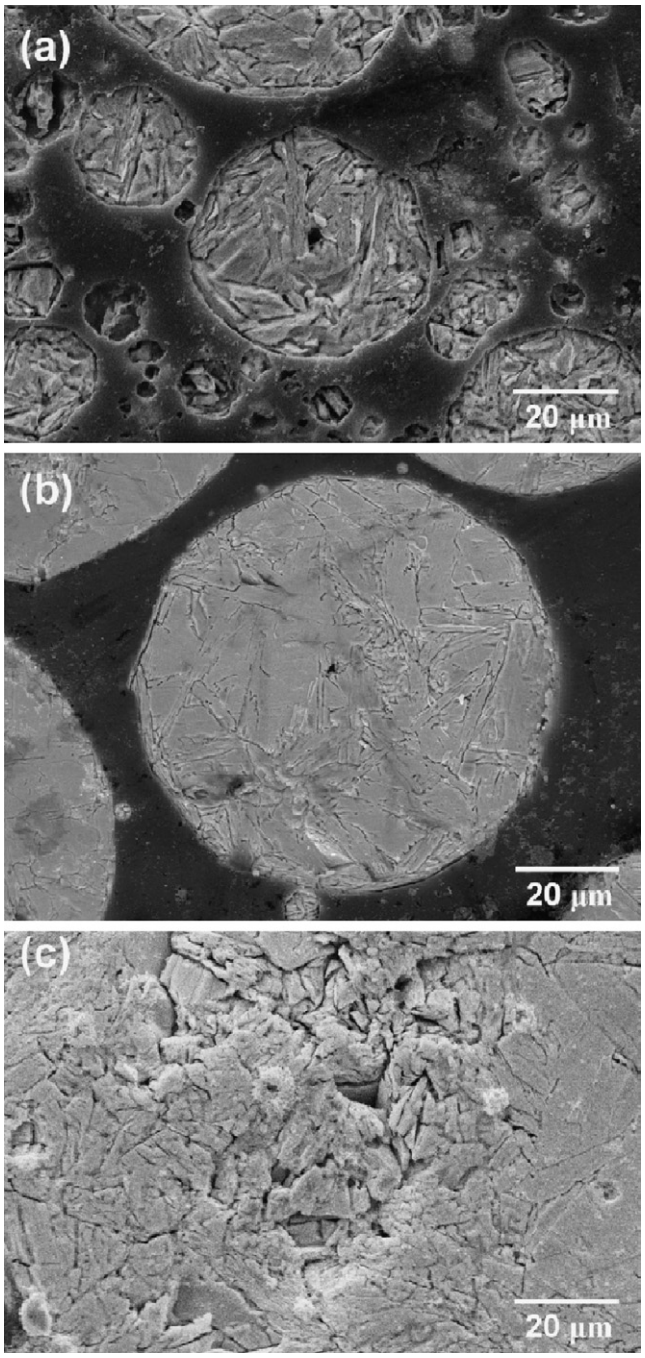

Fig. 5. SEM cross-sectional micrograph of 95% Bi_2Te_3–5% Bi_2Se_3 gas atomized powders; (a) ~45 μm (b) 75–106 μm and (c) 180–250 μm.

large size (180–250 μm) particles, respectively. High cooling rate of the smaller powders suppressed the growth of the intermetallic compounds provided by a large undercooling. The microstructural homogeneity of the powders also depends on the varying undercooling effect at different sections of the powders causing different solidification rates. Hence, rapid solidification of the powders by gas atomization significantly reduced the grain size, and was capable of producing homogeneous and segregation free microstructures compared to the directionally grown single crystals. It can be mentioned that controlling the grain size of the microstructure is one of the key parameters to enhance the figure-of merit. Fine grains in the polycrystalline materials increase the acoustic phonon scatterings by means of grain boundary scattering mechanism, causing to reduce the lattice thermal conductivity, and thus resulting in an increase in the figure-of-merit.

During high temperature processing's such as extrusion and hot pressing of the powders, temperature plays a vital role in determining the microstructure. To examine the effect of high temperature on the microstructure of 95% Bi_2Te_3–5% Bi_2Se_3 gas atomized powders, the as-atomized powders were heat treated at different conditions. A visual outline in the behavior of microstructural change depending on various heat treatment temperatures and holding time for 65–80 μm size powders is exhibited in Figs. 6 and 7. Fig. 6 displays SEM cross-sectional microstructure of the powders heat treated at 300 °C and 500 °C for 1, 3 and 5 h. It seems that the microstructure of the powders was severely affected by the heat treatment temperatures and the holding time as well. Powders heat treated at 300 °C for 1 h (Fig. 6(a)) shows an average grain width of 2.5 μm, and as the holding time was increased to 3 h and 5 h, the average grain size roughly became 4–5 μm (Fig. 6(b)) and 5 μm (Fig. 6(c)), respectively. An increase in holding time from 3 to 5 h did not affect the microstructure much. Meanwhile, powders heat treated at 500 °C for 1 h as shown in Fig. 6(d) reveal a coarse microstructure with an average grain width of 8 μm. Then an increase in holding time up to 3 and 5 h, leads to a rapid and acute coarsening of the grains to around 10 μm (Fig. 6(e)) and 15–16 μm (Fig. 6(f)), respectively. It is evident that microstructural coarsening of the powders occurs more rapidly and effectively at higher heat treatment temperatures and for longer periods.

The consequences of high temperature on the microstructure is further noticeable in Fig. 7, which delineates SEM cross-sectional micrograph of the powders heat treated at 300, 350, 400 and 500 °C for 1 h. It is visible that the average grain width gradually increased from 2.5 μm (Fig. 7(a)) for the powders heat treated at 300 °C to 4.5–6.5 μm and 8 μm for the powders heat treated at 400 °C and 500 °C as shown in Fig. 7(c) and(d), respectively. Whereas, the grain size remained almost constant in case of the powders heat treated at 350 °C (Fig. 7(b)) and 400 °C (Fig. 7(c)). The grain size variation of the powders heat treated at 300, 350, 400 and 500 °C for 1, 3 and 5 h is even more distinct in Fig. 8, which manifests obvious effect on the grain size. From the trajectory, it appears that the average grain width almost proportionally increased with the increasing heat treatment temperatures and holding time. The microstructure coarsening rate accelerates and deviates further from each other at higher temperatures and periods; specifically, it is explicit after the heat treatment temperature of 350 °C. For the powders heat treated at 300 °C, an increase in holding time from 1 to 3 h and 3 to 5 h caused the grain size to grow by 80% and 11%, respectively. Whereas powders heat treated at 500 °C showed a grain growth by 25% and 50%, respectively, for an increase in holding time from 1 to 3 h and 3 to 5 h. Meanwhile, with the increasing heat treatment temperature from 300 to 400 °C and 400 to 500 °C for holding time of 1 h, the grain size was increased by 140% and 33%, respectively. Such a behavior indicates that at lower heat treatment temperatures and periods, a lower fraction of atomic and molecular diffusion takes place. However, after a certain level, the diffusion process accelerates causing a rapid increase in the grain growth, and finally, slows down due to saturated conditions. Investigation of the powder extrusion process [16] discovers that the grain refinement occurs within the microstructure because of the dynamic recrystallization process followed by a grain growth at further higher temperatures. That means, controlling the initial grain size of the powder is important in determining the final microstructure of the bulk. The coarse microstructure increases the carrier mobility (μ) by lowering the carrier scatterings, resulting in an increase in the electrical conductivity (σ) by the relation $\sigma = n_c e\mu$. On the contrary, microstructures having smaller grain size contribute to rise of scattering parameters, which in turn increase the seebeck coefficient. The relationship between the seebeck coef-

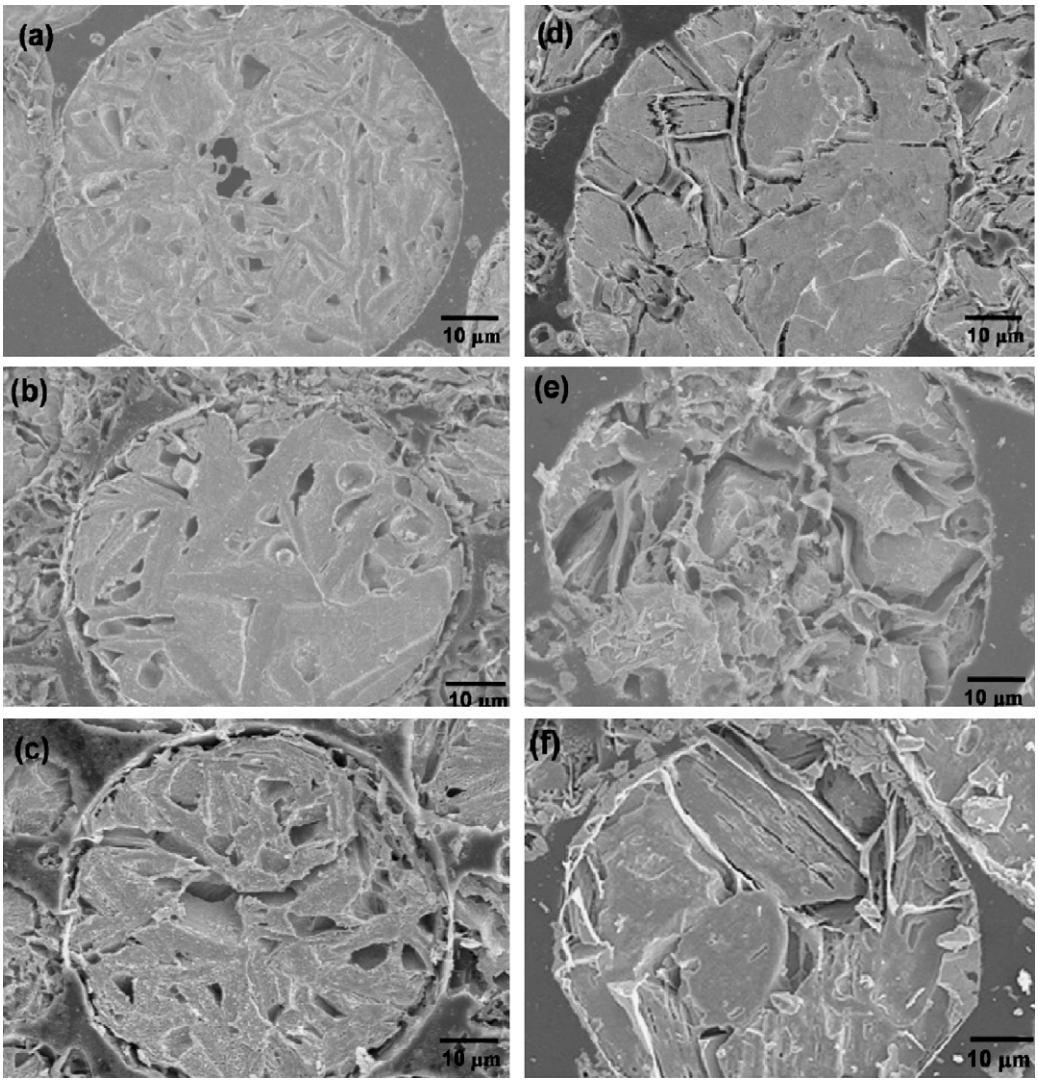

Fig. 6. Cross-sectional microstructure of heat treated 95% Bi_2Te_3–5% Bi_2Se_3 gas atomized powders. (a–c) Heat treated at 300 °C for 1, 3 and 5 h, respectively; (d–f) heat treated at 500 °C for 1, 3 and 5 h, respectively.

ficient (α) and microstructure can be expressed as $\alpha \approx r - \ln(n_c)$, where r is the scattering parameter and n_c is the carrier concentration [17]. Therefore, it refers that to attain a high figure-of-merit (Z), all the thermoelectric parameters of seebeck coefficient (α), electrical conductivity (σ) and thermal conductivity (κ) must be optimized by means of controlling the microstructure.

Due to the nature of the crystal structure, the anisotropy in Bi_2Te_3 system requires preferred orientation of (0 0 6), (0 0 15) and (0 0 18) basal planes along the c-plane to achieve maximum thermoelectric properties. Since powder metallurgy system yields random orientations, statistical distribution of the basal planes is necessary to be calculated in terms of the orientation factor (f). The orientation factor (f) can be calculated by Lotgering method [18] as follows:

$$f = \frac{P - P_o}{1 - P_o}; \quad P = \frac{\sum I(0,0,l)}{\sum I(h,k,l)} \tag{2}$$

where, P is the fractional intensity of the (0 0 l) planes and P_o is the value of P without any preferential orientation (in this case considering the as-atomized powders). Fig. 9 illustrates XRD traces of heat treated 95% Bi_2Te_3–5% Bi_2Se_3 gas atomized powders for various temperatures and holding time. The calculated orientation factors (f) of these powders are shown in Table 1. As can be seen, the maximum orientation factor 0.162 was obtained in the powders heat treated at 300 °C for 1 h. The orientation factor decreases with the increasing heat treatment temperature and holding time, and the decreasing rate gradually slows down at higher heat treatment temperatures and periods. The rapid decrease in orientation factor might be due to higher rate of diffusion of the atoms and molecules at higher heat treatment temperatures and periods. As the orientation factor of the completely oriented and non-oriented material lies between 1.0 and 0.1, therefore, the values in Table 1 suggest that heat treatment of the powders does not significantly affect the orientation factor, rather can be considered as poor orientation of the basal planes relative to the extruded bars (f = 0.24 for extrusion ratio of 25:1) [6]. The surface contaminated oxygen of the particles that might lead to an inferior thermoelectric performance can be reduced by heating the powders in H_2 atmosphere

Table 1
Orientation factors (f) of the heat treated 95% Bi_2Te_3–5% Bi_2Se_3 powders for various temperatures and holding time.

Time (h)	300 °C	400 °C	500 °C
1	0.162	0.096	0.095
3	0.08		
5	0.062		

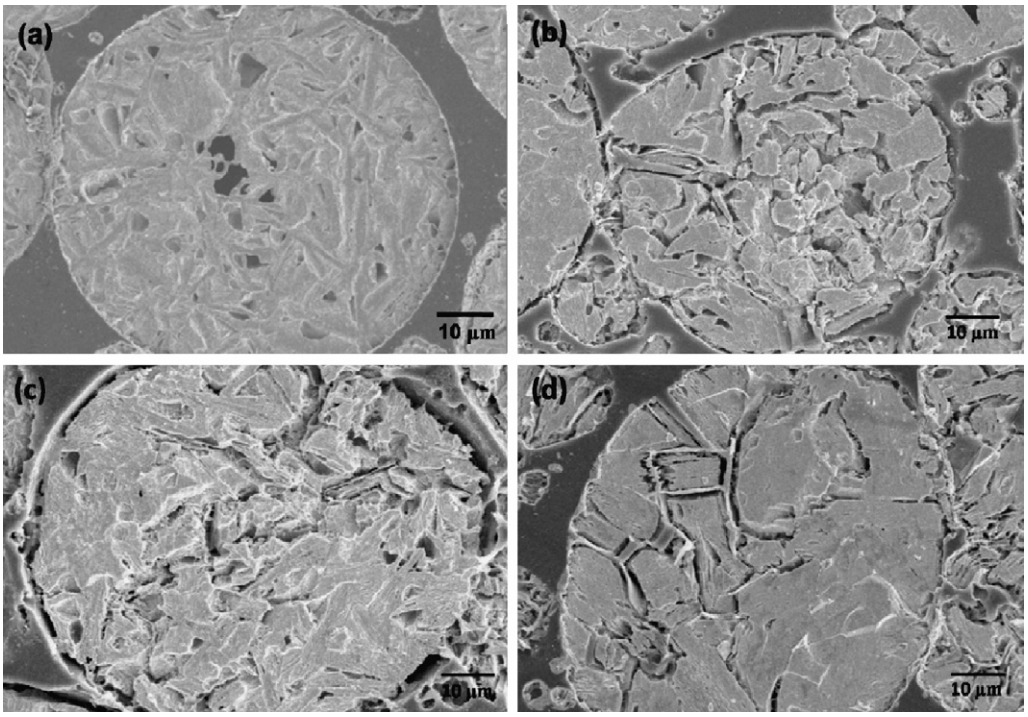

Fig. 7. Cross-sectional microstructure of 95% Bi_2Te_3–5% Bi_2Se_3 gas atomized powders as a function of various heat treatment temperatures for 1 h; (a) 300 °C (b) 350 °C (c) 400 °C and (d) 500 °C.

as a part of the annealing process, which softens the powder for easier compaction. A comparison of the XRD patterns between the as-atomized powders and reduction treated powders is shown in Fig. 10. The calculated orientation factor of the reduction treated powder was 0.044 and showed similar trend to that of the heat treated powders. Fig. 11 represents variation in the Vickers hardness of both non-heat treated and heat treated 95% Bi_2Te_3–5% Bi_2Se_3 gas atomized powders with 65–80 μm size range according to different heat treatment conditions. The average Vickers hardness of the non-heat treated (as atomized) powders was found to be 56.18 Hv. However, hardness of the powders was greatly reduced by the various heat treatment conditions. With the increasing heat treatment temperatures, the Vickers hardness decreased linearly due to microstructural coarsening of the powders as evident in

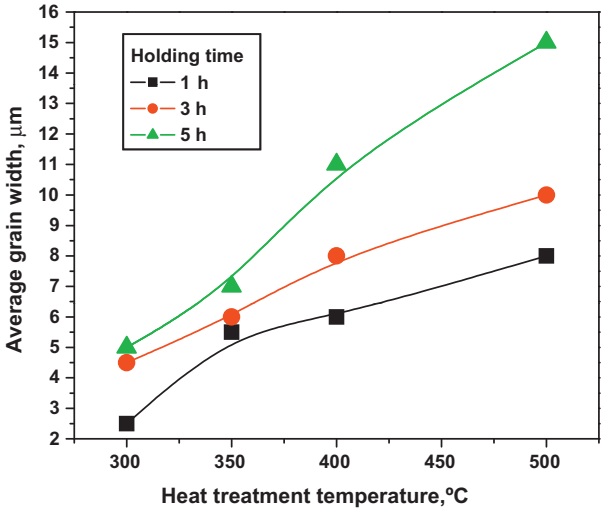

Fig. 8. The variation in grain size of 95% Bi_2Te_3–5% Bi_2Se_3 gas atomized powders at different heat treatment conditions.

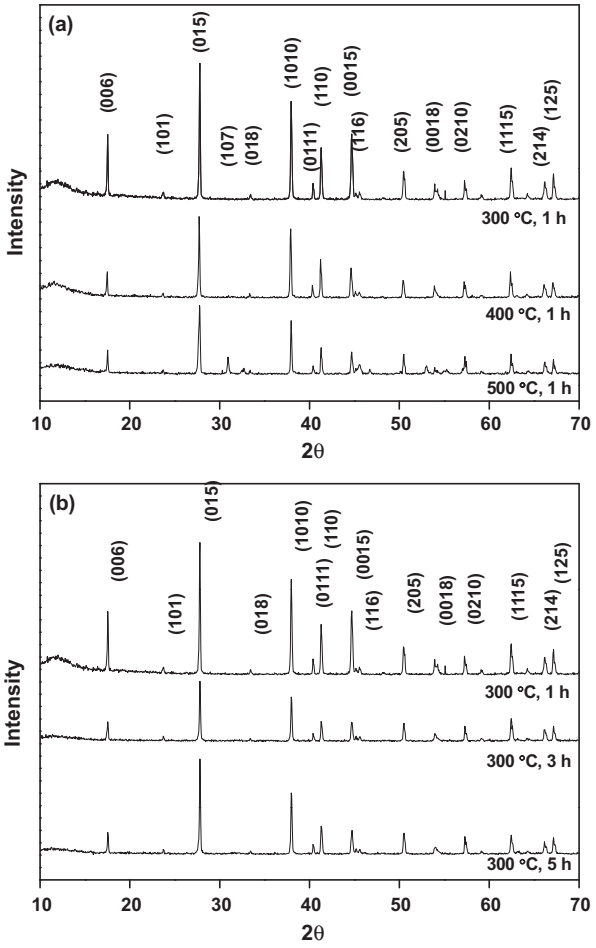

Fig. 9. XRD traces of 95% Bi_2Te_3–5% Bi_2Se_3 powders depending on the heat treatment (a) temperatures and (b) holding time.

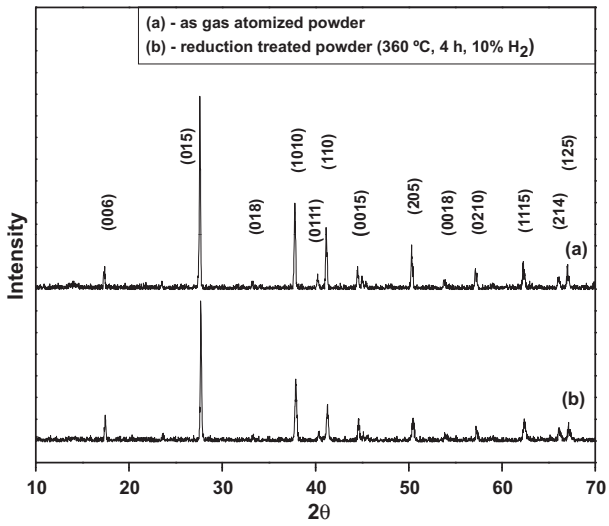

Fig. 10. XRD traces of (a) as atomized and (b) reduction treated 95% Bi_2Te_3–5% Bi_2Se_3 powders.

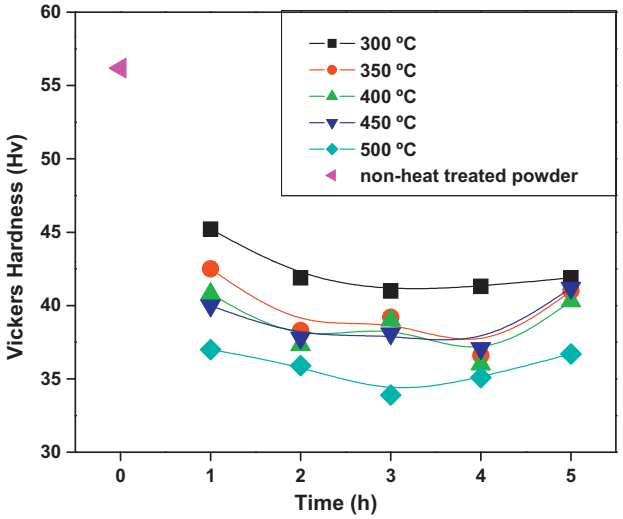

Fig. 11. Variation in the Vickers hardness of 95% Bi_2Te_3–5% Bi_2Se_3 gas atomized powders at different heat treatment conditions.

Fig. 8. In addition, the hardness gradually decreased with some sort of fluctuations as the holding time increased, despite occupying a notable grain growth as shown in Fig. 8. The maximum Vickers hardness of 45.20 Hv was obtained in the powders heat treated at 300 °C for 1 h. This maximum hardness was attained due to the fine grain size of 2.5 μm as observed in Fig. 6(a). The uniform and stable hardness demonstrated by the heat treated powders with respect to the various heat treatment conditions is advantageous and desirable. It is therefore expected that the high hardness of the gas atomized powders would considerably reduce material wastage during the cutting process of the modules. Furthermore, less variation in Vickers hardness (35–45 Hv) of the powders, corresponding to the various heat treatment temperatures and holding time, will also be favorable for stable consolidation of the powders. Hence, gas atomized powders might possess a good combination of mechanical and thermoelectric properties compared to the directionally grown single crystals. In order to further realize the obvious effect of various temperatures and periods on the thermoelectric and mechanical properties of the bulks, the gas atomized 95% Bi_2Te_3–5% Bi_2Se_3 powders will be consolidated at different conditions in future work.

4. Conclusion

The typical rapid solidification process of gas atomization was effective in producing wide range and bimodal size distribution of n-type 95% Bi_2Te_3–5% Bi_2Se_3 doped with 0.04% SbI_3 powders with smooth surface and spherical shape. The as-atomized powders consisted of homogeneously distributed needle shape intermetallic compounds having Bi_2Te_3 phase. The size of the intermetallic compounds decreased with the decreasing powder size, indicating that the grain growth was considerably suppressed by the high cooling rate. The oxygen content in the produced powders increased with the decreasing powder size due to high specific surface area of the smaller powders. Heat treatment of the powders for various temperatures and periods showed a significant increase in the grain size resulting in a reduction in hardness. The rate of grain growth was substantially affected at the later stages of heat treatment by a combination of both temperature and period. The orientation factor of the powder particles decreased with the increasing heat treatment temperatures and periods, which is also evident in case of the reduction treated powders. Vickers hardness of the powders was considerably reduced by the heat treatment conditions owing to the grain size increment. The maximum Vickers hardness of 45 Hv was obtained in the powders heat treated at 300 °C for 1 h, while in case of the non-heat treated powders it was 56 Hv. Hence, microstructural analysis of the heat treated powders will be beneficial in determining powder consolidation temperatures as well as the working time, thus yielding optimum microstructures to obtain an outstanding combination of thermoelectric and mechanical properties in the bulks.

Acknowledgement

This work was supported by Basic Science Research Program through the National Research Foundation of Korea (NRF) funded by the Ministry of Education, Science and Technology (2009-0077468).

References

[1] H.J. Goldsmid, in: D.M. Rowe (Ed.), CRC Handbook of Thermoelectrics, CRC Press Inc., Boca Raton, Florida, 1995, pp. 617–619.
[2] Z. Ding, S.C. Huang, D. Marcus, R.B. Kaner, 18th International Conference on Thermoelectrics, 29 August–2 September, 1999, pp. 721–724.
[3] S. Nakajima, J. Phys. Chem. Solids 24 (3) (1963) 479–485.
[4] H.J. Goldsmid, J. Appl. Phys. 32 (10) (1961) 2198–2202.
[5] M. Carle, P. Pierrat, C. Lahalle-Gravier, S. Scherrer, H. Scherrer, J. Phys. Chem. Solids 56 (2) (1995) 201–209.
[6] S.J. Hong, S.H. Lee, B.S. Chun, Mater. Sci. Eng. B 98 (2003) 232–238.
[7] M. Takashiri, T. Shirakawa, K. Miyazaki, H. Tsukamoto, Sens. Actuators A 138 (2007) 329–334.
[8] J.Y. Yang, T. Aizawa, A. Yamamato, T. Ohta, J. Alloys Compd. 312 (2000) 326–330.
[9] Y. Deng, X. Zhou, G. Wei, J. Liu, C. Nan, S. Zhao, J. Phys. Chem. Solids 63 (2002) 2119–2121.
[10] J. Jiang, L. chen, S. Bai, Q. Yao, Q. Wang, Mater. Sci. Eng B117 (2005) 334–338.
[11] X.A. Fan, J.Y. Yang, W. Zhu, H.S. Yun, R.G. Chen, S.Q. Bao, X.K. Duan, J. Alloys Compd. 420 (2006) 256–259.
[12] R.M. German, Powder Metallurgy Science, second ed., Metal Powder Industries Federation, New Jersy, 1997, p. 168.
[13] B.A. Cook, J.L. Harringa, S.H. Han, B.J. Beaudry, J. Appl. Phys. 72 (1992) 1423.
[14] E.L. Kukharenko, V.G. Shepelevich, Inorg. Mater. 35 (2) (1999) 115–117.
[15] T.S. Kim, I.S. Kim, T.K. Kim, S.J. Hong, B.S. Chun, Mater. Sci. Eng. B 90 (2002) 42–46.
[16] S.J. Hong, B.S. Chun, Mater. Sci. Eng. A 356 (2003) 345–351.
[17] A.F. Ioffe, Semiconductor Thermoelement and Thermoelectric Cooling, Infosearch Ltd., London, 1957.
[18] F.K. Lotgering, J. Inorg. Nucl. Chem. 9 (2) (1959) 113–123.